MALAYSIAN JOURNAL OF SCIENCE
MJS
ISSN 1394-3065

Regular Issue

Malaysian Journal of Science 43 (3): 22-29 (September 2024) https://mjs.um.edu.my

GREEN ROUTE SYNTHESIS OF COPPER OXIDE (CuO) NANOPARTICLES FOR THE DEGRADATION OF COMMERCIAL DYES USING *VICIA FABA* LEAF EXTRACT

P. Rastogi[1a], P. Negi[2b]*, B. S. Rawat[3a], N. C. Joshi[4d]

Abstract: The release of toxic dyes into water effluents by various industries has become a global concern. Therefore, developing novel, straightforward, and economically viable methods or materials for purifying these hazardous pigments is imperative. This study aims to synthesize copper oxide nanoparticles (CuO-NPs) through a green route using *Vicia faba* leaf extract. UV-Vis spectroscopy reveals an absorption band ranging from 200 nm to 300 nm, with a major absorption peak at 212 nm and an energy band gap of 5.29 eV. FTIR, SEM, EDX, and XRD techniques characterise the synthesised CuO nanoparticles. FTIR analysis identifies functional groups including hydroxyl (OH), aromatic C-H, C=C stretching, carbonyl (C=O), and Cu-O stretching vibrations. Scanning electron microscopy reveals flower-like particles, while EDX analysis confirms the formation of CuO nanoparticles. The XRD pattern indicates a crystalline structure with an average particle size of 27.44 nm. A plot of $(\alpha h\nu)^2$ versus photon energy (hv) was generated to determine the energy band gap, yielding a value of 5.29 eV. Rhodamine-B and methylene blue (MB) dyes were employed to evaluate the photocatalytic degradation of the synthesized CuO-NPs, resulting in correlation coefficients of 0.7154and 0.9702, respectively. Furthermore, the rate constants of these dye reactions were found to be 0.0406min^{-1} and0.0343 min^{-1}.

Keywords: *nanoparticles, photocatalytic degradation, Vicia faba, methylene blue, rhodamine-B.*

1. Introduction

Industrial and household wastewater effluents pose significant threats to both human health and aquatic life (Joshi et al. 2022). Industrial effluents may contain hazardous substances, including pesticides, unprocessed colored dyes, and organic dyes. Upon exposure to sunlight, organic dyes undergo photocatalysis, reducing the dissolved oxygen in water. The absorption of sunlight by dye molecules generates highly reactive oxygen species, which react with oxygen molecules and contaminants, leading to a depletion of dissolved oxygen levels. Moreover, dyes can form complexes with oxygen, hindering its dissolution in water and further reducing the availability of oxygen for aquatic life (Dutta et al. 2021; Farré et al. 2008). The widespread use of industrial dyes in the paper, pharmaceutical, textile, and leather industries negatively impacts water resources and disrupts aquatic ecosystems. Consequently, it is crucial to remove these toxic dyes from the environment.

Various strategies have been considered for the treatment of the harmful substances. However, these methods often only change the phase of the contaminants rather than completely degrading them. To address these challenges, nanostructures have been explored for their potential to degrade dyes (Kumar et al. 2018). These nanostructures include metal oxide nanoparticles, zeolites, nanorods, and others (Sharma et al. 2017). The use of metal oxide nanoparticles has proven to be one of the most effective and promising methods for removing hazardous contaminants from water (Anjum et al. 2016). Nanoparticles offer several advantages, and their production can be achieved through various methods, including chemical processes. However, the use of harmful toxic chemicals and certain processes in chemical methods cannot be ignored. Given that metal nanoparticles come into contact with the human body, there is a pressing need to develop eco-friendlier methods, such as biological synthesis, to mitigate the detrimental effects of chemical nanoparticle synthesis protocols. Biological synthesis involves the extraction of nanoparticles from plant material, microorganisms, and enzymes (Asemani et al. 2019).

Copper nanoparticles are of great importance due to their applications in gas sensors, lubricants, superconductors, and dye-sensitized solar cells (Mandke et al. 2012). Copper oxide nanoparticles also possess significant biological properties, including antifouling, antimicrobial, and antifungal activities (Crisan et al. 2022). Several methods can be employed to synthesize copper oxide nanoparticles, including chemical reduction, microwave irradiation, and electrochemical methods (Mandke et al. 2012; Dang et al. 2011; Naveena et al. 2022). With increasing awareness, there is a growing focus on the development of eco-friendly synthesis methods for nanoparticles. The use of plants, microorganisms, and enzymes for synthesizing non-toxic, biologically benign metal nanoparticles is gaining importance (Kulkarni et al. 2014). The phyto constituents present in plants and microorganisms mediate the synthesis of nanoparticles by acting as capping agents.

Authors information:
[a]Department of Physics, School of Applied and Life Sciences (SALS), Uttaranchal University, Dehradun-248007, UK, INDIA.
[b]Department of Chemistry, GRD Institute of Management & Technology, Dehradun, UK, INDIA.
[c]Division of Research and Innovation, Uttaranchal University, Dehradun-248007, UK, INDIA.
*Corresponding Author: park_bhupendra@hotmail.com

Received: March 16, 2023
Accepted: September 29, 2023
Published: September 30, 2024

DOI:https//doi.org/10.22452/mjs.vol43no3.3
Malaysian Journal of Science 43(3): 22-29 (September 2024)

Vicia faba is an erect, rigid annual legume that is widely cultivated in most parts of the world. Its leaves are 8-15 cm long and grey-green in color (Singh et al. 2013). The bean plant exhibits several medicinal properties, including antidiabetic, diuretic, and antihypertensive effects, and can also fix atmospheric nitrogen (Köpke et al. 2010). Moreover, it is a rich source of phenolic compounds (Valente et al. 2018).

The current study aims to synthesize copper oxide nanoparticles using a green synthesis method with aqueous *Vicia faba* leaf extract and subsequently use these nanoparticles to degrade harmful dyes such as Rhodamine-B and methylene blue.

2. Materials and Method

Analytical-grade chemicals, including copper (II) sulfate pentahydrate, Rhodamine-B (Rh-B), and methylene blue (MB), were utilized in this study. The leaves of *Vicia faba* were collected from the local region of Dehradun in March. The Agricultural Department of Uttaranchal University authenticated the collected plant material.

Fresh, healthy plant leaves were thoroughly washed with double-distilled water to remove contaminants. After drying in the shade for five days to eliminate moisture, the plant material was finely ground into a powder. Subsequently, 500 ml of deionized water was mixed with 20 g of powdered plant material on a magnetic stirrer with ahot plate at 65°C for eight hours. The resulting extract was then filtered using Whatman filter paper.

3. Synthesis of CuO-NPs

Copper oxide nanoparticles (CuO-NPs) were synthesized from *Vicia faba* by mixing 1 mM copper sulfate with10g of the extract. The mixture was then combined with a 1 M NaOH solution to achieve a pH of approximately 8. The solution was stirred with a magnetic stirrer for 10 hours at 40°C. Subsequently, the solution containing the precipitate was centrifuged, and the precipitate was separated and transferred to a Petri dish. It was then dried in a hot air oven at 100°C. After drying, the precipitate was finely powdered and stored in a vial for further characterization (Fig. 1).

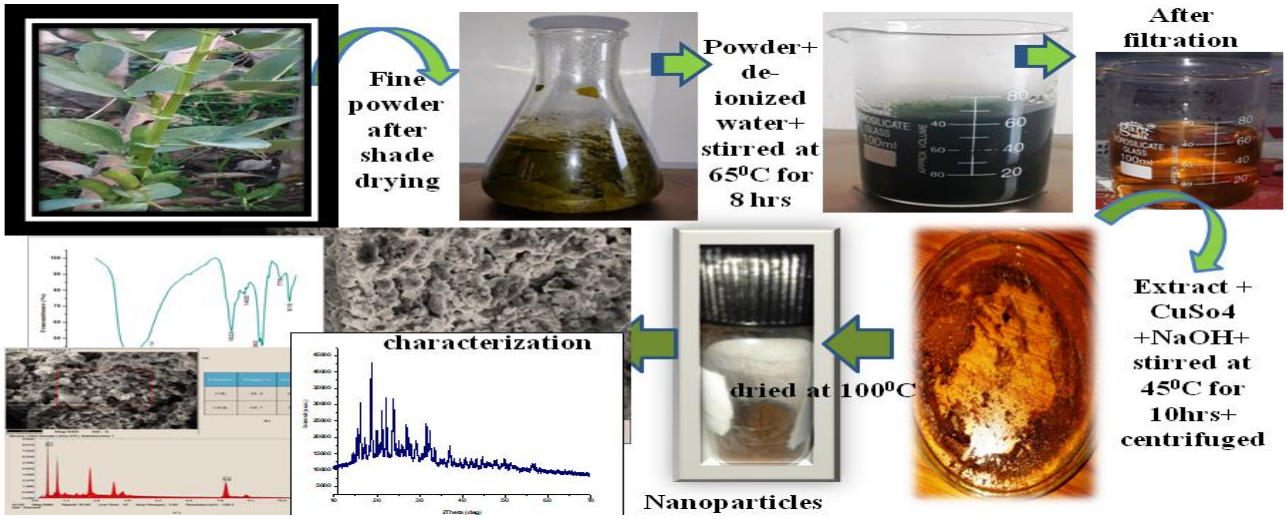

Figure 1. Scheme for the synthesis of CuO-NPs

DOI:https//doi.org/10.22452/mjs.vol43no3.3
Malaysian Journal of Science 43(3): 22-29 (September 2024)

4. Results and Discussion

SEM & EDX Analysis

SEM analyses were employed to characterize the morphology of CuO-NPs. However, due to the sample preparation process, the SEM analysis revealed the presence of agglomerated particles with a roughly flower-like shape (Fig. 2).

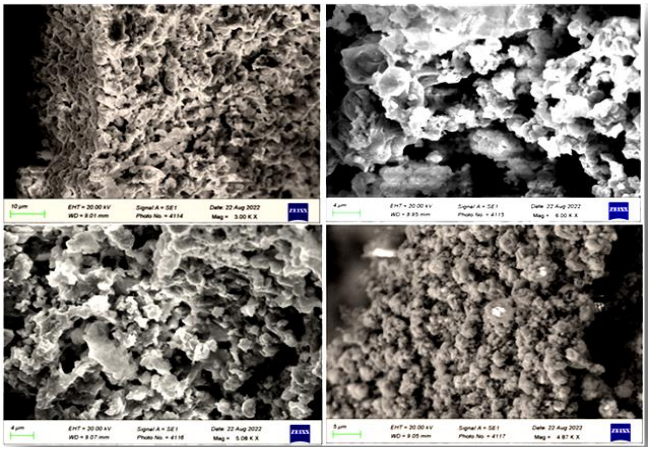

Figure 2. SEM morphology of nanoparticles

For confirmation of the elements present in CuO-NPs, EDX analysis was conducted (Fig. 3). The EDX results revealed the presence of characteristic copper and oxygen, with weight percentages of 68.7% and 31.3%, respectively, and intensity peak values of 4353.1 and 5997.3. These results confirm the successful synthesis of CuO-NPs using the *Vicia faba* leaf extract. It is noteworthy that the additional peaks observed in the EDX analysis may be attributed to the presence of organic groups, which could potentially be removed by washing the extract with ethanol and distilled water.

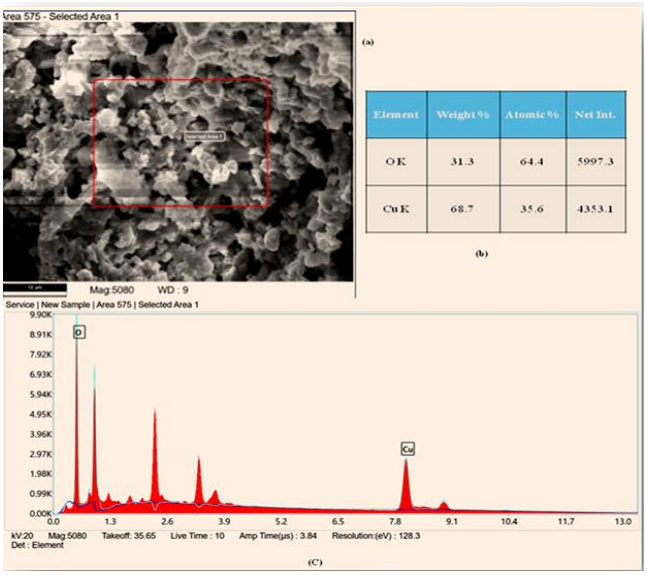

Figure 3. EDX spectrum of nanoparticles

FT-IR Analysis

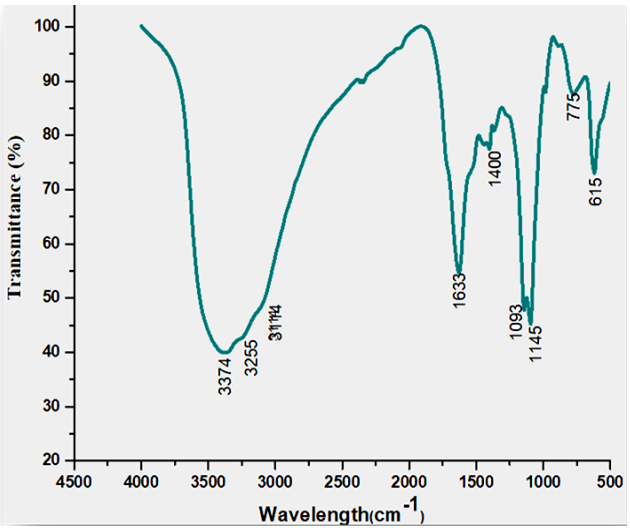

Figure 4. FT-IR spectra of synthesized nanoparticles

FTIR analysis was conducted to identify the various functional groups in volvedin the Nanoparticles (Fig.4).Thespectraobtained from the *Vicia faba* leaf extract exhibited distinct bands at 3374cm^{-1}, 3255cm^{-1}, 3114cm^{-1}, 1633cm^{-1}, 1400cm^{-1}, 1145cm^{-1}, 1093cm^{-1}, 775cm^{-1}, and 615 cm^{-1}. The prominent peak at 3374 cm^{-1} indicated the presence of a hydroxyl (OH) functional group, commonly found in alcohols and phenolic compounds (Rajendran et al., 2022). The band at 3114 cm^{-1} can be attributed to the stretching vibrations of aromatic C-H bonds, while the absorption band at 1400 cm^{-1} is due to the fundamental vibrations of aromatic C=C bonds (alkene group). The presence of a carbonyl (C=O) group is suggested by a dip near 1633 cm^{-1}, and the absorption band around 1093 cm^{-1} indicates Cu-O stretching vibrations. Additionally, the smaller peaks observed in the 775-615 cm^{-1} range are attributed to the bending vibrations of aromatic C-H bonds out of the plane. These findings suggest that flavonoids and other phenolic compounds in the *Vicia faba* leaf extract play a stabilizing role on the surface of the produced metal oxide nanoparticles. This stabilization contributes to their reducing properties and facilitates the reduction of Cu^{2+} ions to form CuO-NPs.

XRD Analysis

X-ray Diffraction (XRD) analysis (Fig. 5) of the synthesized CuO nanoparticles confirms their crystalline structure. The XRD pattern exhibits distinct diffraction peaks at 2θ angles of approximately 35.48°, 38.65°, 46.08°, 48.74°, 58.22°, 61.51°, 66.22°, 67.98°, and 75.01°, corresponding to the lattice planes (111), (111), (112), (202), (202), (113), (311), (113), and (004), respectively. These results from the XRD spectrum provide strong evidence for the presence of copper oxide nanoparticles, and their structural characteristics are consistent with the SEM image.

DOI:https//doi.org/10.22452/mjs.vol43no3.3
Malaysian Journal of Science 43(3): 22-29 (September 2024)

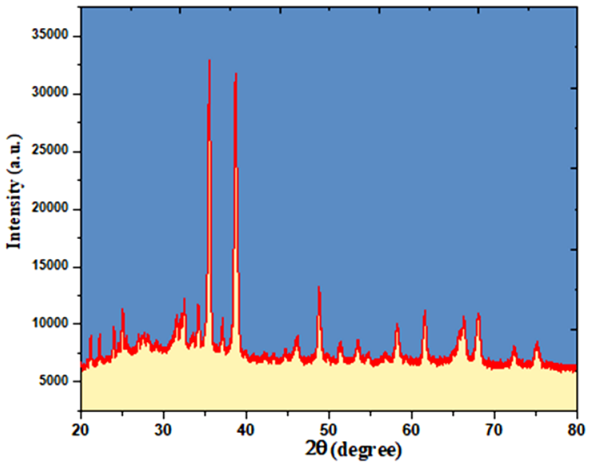

Figure 5. XRD Spectrum of synthesized nanoparticles

Table 1 presents the assigned peak values (2θ), d-spacing values, relative intensity, and particle size estimation of the particles. The Debye-Scherrer equation, detailed below, was used to evaluate the particle size, which was determined to be 27.44 nm (Jenkins et al., 1996). The Scherrer constant and X-ray wavelength were set at 0.89 and 0.15418, respectively. Furthermore, the indexed peak values were compared with the standard card for the anatase phase of the powder sample (JCPDS card no: 01-080-1916), confirming a match.

Table 1. Average particle size, d-spacing and lattice parameters

Peak position (2θ)	Peak height (cts)	Full width half max (2θ)	d-spacing [Å]	Relative Intensity (%)	hkl	Particle size [Å]
35.4890	32719.89	0.295	2.47	100.00	111	291
38.6470	31706.50	0.236	2.27	96.90	111	369
46.0810	8800.19	0.472	1.92	26.90	112	186
48.7390	13178.78	0.276	1.82	40.28	202	325
58.2240	9899.62	0.394	1.55	30.26	202	236
61.5060	11161.57	0.315	1.47	34.11	-113	301
66.2220	10482.79	0.315	1.38	32.04	-311	309
67.9830	10740.92	0.354	1.35	32.83	113	277
75.0110	8217.02	0.768	1.24	25.11	004	176

Optical Properties Analysis

A UV-visible spectrophotometer at room temperature was employed for investigating the absorption peaks, range of the absorption spectrum, and energy band gap (Fig 6).

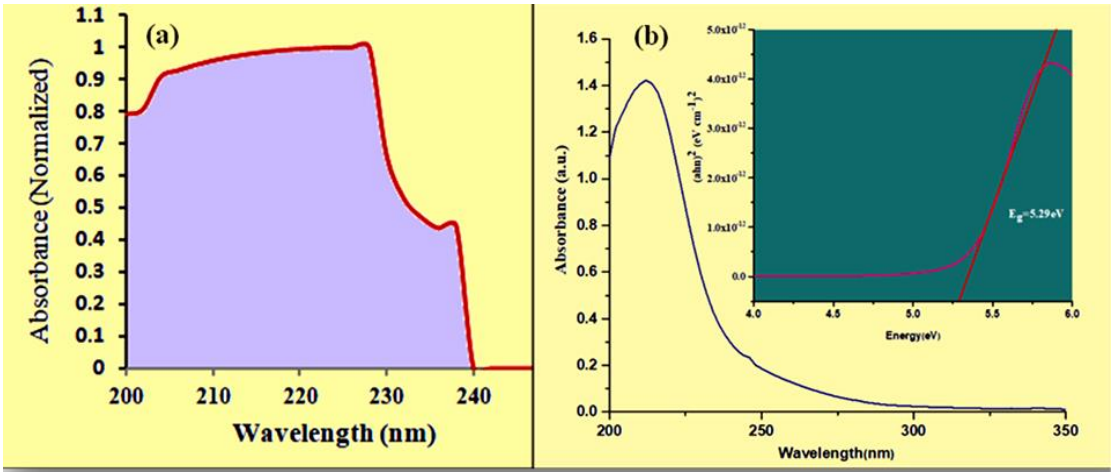

Figure 6. Plot of absorbance against wavelength of (a) *Vicia faba* leaves extract and (b) *Vicia faba* CuO-NPs along with $(\alpha hv)^2$versushv

DOI:https//doi.org/10.22452/mjs.vol43no3.3
Malaysian Journal of Science 43(3): 22-29 (September 2024)

The absorption spectrum of *Vicia faba*leaf extract was observed in the range from 200 nm to 240 nm, displaying distinct peaks at 204 nm, 228 nm, and 238 nm. In contrast, the absorption spectrum of *Vicia faba* CuO-NPs spanned a broader range from 200 nm to 300 nm, with a prominent peak at 212 nm. The presence of multiple peaks in the plant extract spectrum may be attributed to various compounds with different absorption properties. Additionally, the pronounced peak at 212 nm confirms the successful formation of CuO-NPs. To ensure consistency in examining the absorption spectra, ethanol was used as the solvent for both the plant extract and CuO-NPs.

Considering the absorption edge, the indirect optical energy band gap was estimated from the absorption spectrum. Tauc's equation was employed for this estimation, supported by existing literature (Muhammad et al., 2011; Yakuphanoglu et al., 2005). The energy band gap value was determined by plotting $(\alpha hv)^2$ versus photon energy (hv), yielding a value of 5.29 eV. The relationship between the absorption coefficient (α) and the energy of the incident photon (hv) is given by the equation mentioned below (Tauc et al., 1996).

$$\alpha hv = \alpha_0 \left(hv - E_g\right)^n$$

where E_g is the energy band gap, v is the incident photon frequency, α_0 is the energy independent constant, and n defines the type and nature of transitions.

Investigation of Photocatalytic Potential

To evaluate the photocatalytic activity of CuO-NPs, the degradation of Methylene blue (MB) and Rhodamine-B (Rh-B) dyes in aqueous solutions was examined. The mechanism for the decomposition of these dyes on the surface of CuO-NPs is detailed in the literature (Devi & Singh, 2014).

Standard solutions with a concentration of 20 mg/L for both Rhodamine-B and Methylene blue dyes were prepared. Each standard dye solution (10 ml) was mixed with 1 mg to 13 mg of CuO-NPs, at 2 mg intervals, in separate test tubes. The solutions were then exposed to direct sunlight with an intensity of 9.2 W/m². The absorption spectra were analyzed using a UV-visible spectrophotometer at 663 nm for MB and 547 nm for Rh-B, with measurements taken at 15-minute intervals. The photocatalytic degradation efficiency (PDE) was calculated using the formula (Chen et al., 2015):

PDE (%) = [Initial concentration of dye (C_o) – remaining dye concentration after time t (C)x100]/ Initial concentration of dye (C_o)

The degradation of the aqueous solution under sunlight exposure was investigated, and the results are presented in Figures 7(a) and 8(a) for Rh-B and MB dyes, respectively. The suspensions of CuO-NPs were separated by taking 3 mL aliquots and subjecting them to centrifugation. MB was completely decomposed within 105 minutes in the presence of CuO-NPs as the catalyst, while Rh-B was degraded within 75 minutes.

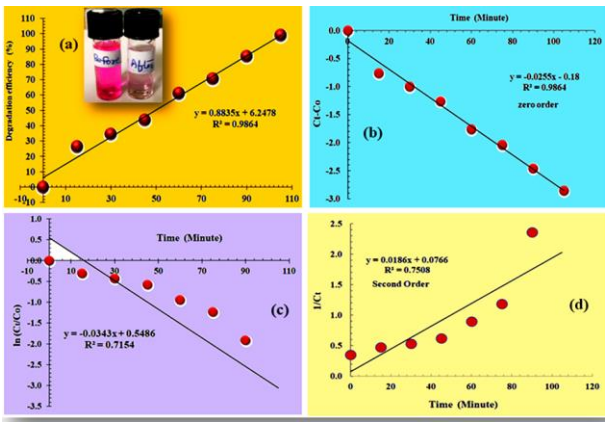

Figure 7(a). Photocatalytic degradation efficiency of Rh-B **Figure 7(b-d).**Kinetic results for the degradation of Rh-B

Additionally, degradation was confirmed by recording absorption spectra at 663 nm for MB and 547 nm for Rh-B dye. According to Sharma and Dutta (Sharma et al., 2015), hydroxyl radicals are identified as the primary reactive oxygen species responsible for the degradation process. Furthermore, the kinetics of the selected dyes' photocatalytic degradation were investigated and presented in Figure 7(b) for Rh-B and Figure 8(b) for MB dye.

To determine the kinetic rate of the reaction, the experimental results were analyzed using zero-order, first-order, and second-order reaction kinetics, as outlined by Mukhlish et al. (2013).

$$C_t - C_o = -k_o t, zero\ order (1)$$

$$\ln(C_t/C_o) = -k_1, First\ order (2)$$

$$1/C_t = k_2 t, Second\ order (3)$$

From the table (Table 2), it can be predicted that for Rh-B, the coefficient of determination (R^2) is higher for the zero-order reaction (0.9864) compared to the first-order (0.7154) and second-order (0.7508) reactions. Conversely, for MB, the first-order reaction exhibits the highest R^2 (0.9702) compared to the zero-order (0.9501) and second-order (0.8225) reactions.

Furthermore, the rate constants for Rh-B are 0.0255 min^{-1} (zero-order), 0.0343 min^{-1} (first-order), and 0.0186 min^{-1} (second-order). For MB, the rate constants are 0.0124 min^{-1} (zero-order), 0.0406 min^{-1} (first-order), and 0.1298 min^{-1} (second-order). These results suggest that the discoloration of Rh-B and MB dyes can be primarily explained by zero-order and first-order reactions, respectively.

DOI:https//doi.org/10.22452/mjs.vol43no3.3
Malaysian Journal of Science 43(3): 22-29 (September 2024)

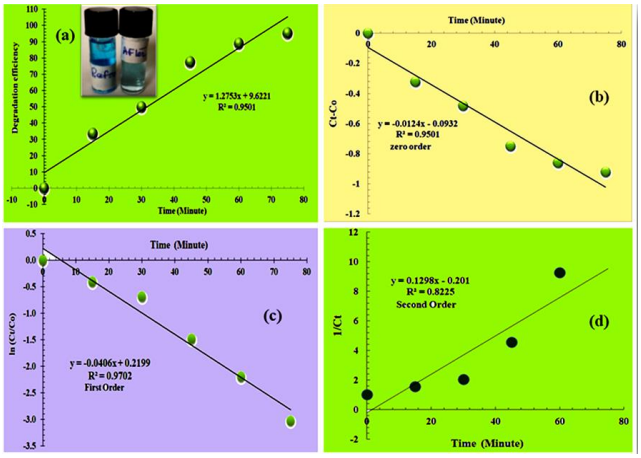

Figure 8(a). Photocatalytic degradation efficiencyof MB**Figure 8(b-d).** Kinetic results for the degradation of MB

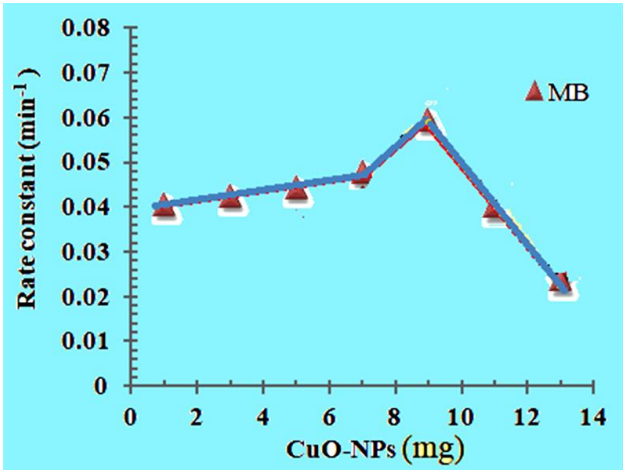

Figure 9. Photocatalytic degradation rate constant variation of MB under the effect of CuO-NPs load

Figure 9 illustrates the variation in the rate constant (min^{-1}) of MB at different amounts (mg) of CuO-NPs extracted from *Vicia faba* leaves. The experiments maintained a constant dye concentration, as previously mentioned. The results indicate an initial gradual increase in the rate constant up to 9 mg/10 ml, followed by a subsequent faster decrease. The examination of the rate constant (min^{-1}) for Rh-B is not considered with different amounts, as it remains constant for the zero-order reaction over time and is not affected by changes in reactant concentration.

The enhanced degradation efficiency of the MB dye with an increasing amount of CuO-NPs catalyst can be attributed to the greater availability of active sites on the catalyst's surface, which accelerates the formation rates of radicals. However, when the catalyst amount exceeds 9 mg/10 ml, the rate constant decreases due to light scattering and reduced light penetration through the solution. At higher catalyst loadings, the deactivation of activated molecules by collisions with ground-state molecules becomes more dominant in the reaction, leading to a reduced reaction rate (Neppolian et al., 2001).

Table 2. Parameters used and results of kinetic of degradation of dyes.

Parameters	Dye	
	Rh-B	**MB**
Solution	aqueous	aqueous
equation of kinetics	y = -0.0255x - 0.18 (zero-order) y = -0.0343x + 0.5486 (first-order) y= 0.0186x + 0.0766(second-order)	y = -0.0124x - 0.0932 (zero-order) y = -0.0406x + 0.2199 (first-order) y = 0.1298x - 0.201 (second-order)
correlation coefficient (R^2)	R^2 = 0.9864(zero-order) R^2 = 0.7154(first-order) R^2 = 0.7508 (second-order)	R^2 = 0.9501 (zero-order) R^2 = 0.9702 (first-order) R^2 = 0.8225 (second-order)
rate constant of reaction	0.0255min^{-1}(zero-order) 0.0343 (first-order) 0.0186 (second-order)	0.0124 min^{-1} (zero-order) 0.0406 min^{-1} (first-order) 0.1298 min^{-1} (second-order)

5. Conclusion

In the present study, *Vicia faba* leaf extract was effectively utilized to synthesize CuO nanoparticles (CuO-NPs), which exhibited a flower-shaped morphology with an average size of 27.44 nm. The formation of CuO-NPs was confirmed through absorption spectrum analysis, and the crystalline structure of the synthesized nanoparticles was validated using X-ray diffraction (XRD).

The synthesized CuO-NPs were employed in the degradation of Methylene Blue (MB) and Rhodamine B (Rh-B) dyes, with notable efficacy observed, particularly in the case of Methylene Blue.

Based on the present findings, it can be concluded that the green synthesis of nanoparticles using *Vicia faba* leaf extract represents an environmentally friendly approach, as it does not release secondary chemical by products. Furthermore, these nanoparticles have demonstrated their suitability for the degradation of toxic industrial dyes.

6. Funding

The present work was carried out with the support of seed money (Ref: UU/DRI/SM/2022/13) provided by Uttaranchal University, Dehradun.

DOI:https//doi.org/10.22452/mjs.vol43no3.3
Malaysian Journal of Science 43(3): 22-29 (September 2024)

7. Acknowledgement

Dr. B.S. Rawat, one of the contributors, expresses gratitude to the Division of research & Innovation, Uttaranchal University, Dehradun for facilitating the research facilities.

8. Conflicts of Interest

The author(s) declare(s) that there is no conflict of interest regarding the publication of this paper.

9. References

Anjum, M., Miandad, R., Waqas, M., Gehany, F., Barakat, M.A. (2016). Remediation of wastewater using various nano-materials. Arab. J. Chem, doi:10.1016/j.arabjc.2016.10.004

Asemani, M., Anarjan, N. (2019). Green synthesis of copper oxide nanoparticles using *JUGLANS REGIA* leaf extract and assessment of their physico-chemical and biological properties. Green Processing and Synthesis, 8 (1), 557-567. doi.org/10.1515/gps-2019-00252011.

Chen, W., Zheng, L., Jia, R., Wang, N. (2015). Cloning and expression of a new manganese peroxidase from Irpex lacteus F17and its application in decolorization of reactive black 5. Process Biochemistry, 50(11), 1748–1759.

Crisan, M.C., Teodora, M., and Lucian, M. (2022). Copper Nanoparticles: Synthesis and Characterization, Physiology, Toxicity and Antimicrobial Applications. Appl. Sci.., *12*(1), 141; https://doi.org/10.3390/app12010141

Dang, T.M.D., Le, T.T.T., Fribourg-Blanc, E., Dang, M.C. (2011). Synthesis and optical properties of copper nanoparticles prepared by a chemical reduction method. Adv Nat Sci: Nanosci Nanotechnol 2(1):015009. doi 10.1088/2043-6262/2/1/015009

Devi, H. S., Singh, T. D. (2014). Synthesis of copper oxide nanoparticles by a novel method and its application in thedegradation of Methyl orange. Advance in Electronic and Electric Engineering, 4(1), 83–88.

Dutta, S., Banerjee, P., Das, P., Mukhopadhyay, A. (2021). Phytogenic synthesis of nanoparticles and their application in photo catalysis of dye rich effluents, Photocatalytic Degradation of Dyes, Elsevier, 647-694

Farré, M. la, Pérez, S., Kantiani, L., Barceló, D. (2008). Fate and toxicity of emerging pollutants, their metabolites and transformation products in the aquatic environment. TrAC-Trends Anal. Chem, 27, 991–1007. doi:10.1016/j.trac.2008.09.010

Jenkins, R., Snyder, R. L. (1996). Introduction to X-Ray Powder Diffractometry, (1st ed). New York, USA, John Wiley and Sons, 554.

Joshi, N.C., Gururani, P., Gairola, S.P. (2022). Metal Oxide Nanoparticles and their Nanocompositebased Materials as Photocatalysts in the Degradation of Dyes. Biointerface Research in Applied Chemistry, 12(5), 6557-6579. doi.org/10.33263/BRIAC125.65576579

Köpke, U., Nemecek, T. (2010). Ecological services of faba bean. Field Crops Research, 115, 217–233. doi.org/10.1016/j.fcr.2009.10.012

Kulkarni, N., and Muddapur, U. (2014). Biosynthesis of Metal Nanoparticles: A Review, Journal of Nanotechnology, Article ID 510246, 8 pages http://dx.doi.org/10.1155/2014/510246

Kumar, M., Mehta, A., Mishra, A., Singh, J., Rawat, M., Basu, S. (2018). Biosynthesis of tin oxide nanoparticles using Psidium Guajava leave extract for photocatalytic dye degradation under sunlight. Mater. Lett, 215, 121–124. doi.org/10.1016/j.matlet.2017.12.07

Mandke, M.V., Pathan, H.M. (2012). Electrochemical growth of copper nanoparticles: structural and optical properties. J Electroanal Chem, 686, 19–24. doi.org/10.1016/j.jelechem.2012.09.004

Muhammad, F.F., Sulaiman, K. (2011). Utilizing a simple and reliable method to investigate the optical functions of small molecular organic flms-Alq3 and Gaq3 as examples. Measurement, 44(8), 1468–1474. doi.org/10.1016/j.measurement.2011.05.017

Mukhlish, M. B., Najnin, F., Rahman, M. M., Uddin, M. J. (2013). Photocatalytic degradation of different dyes using TiO2 withhigh surface area: a kinetic study. Journal of Scientific Research, 5(2), 301–314.

Naveena, D., Dhanabal, R., Bose, A. C. (2022). Investigating the effect of La doped CuO thin film as absorber material for solar cell application.Optical Materials, Volume 127, 112266. doi.org/10.1016/j.optmat.2022.112266

R. Singh, R., Dutta,S. (2018). Synthesis and characterization of solar photoactive TiO_2 nanoparticles with enhanced structural and optical properties, Adv. Powder Technol, 29 211–219, doi:http://dx.doi.org/10.1016/j.apt.2017.11.005.

Rajendran, R., Pullani, S., Thavamurugan, S., Radhika, R., Prabha, A.L. (2022). Green Fabrication of silver nanoparticles from Salvia species extracts: characterization and anticancer activities against A549 human lung cancer cell line. Applied Nanoscience, 5(7),1515-1519. https://doi.org/10.1007/s13204-021-02130w.

DOI:https//doi.org/10.22452/mjs.vol43no3.3
Malaysian Journal of Science 43(3): 22-29 (September 2024)

Sharma, R., Dutta, K. (2015).Studies on the drastic improvement of photocatalytic degradation of acid orange-74 dye by TPPO capped CuO nanoparticles in tandem with suitable electron capturingagents, RSCAdv. 5, 43815–43823, doi:http://dx.doi.org/10.1039/c5ra04179a.

Sharma, V.K., Feng, M. (2017). Water depollution using metal-organic frameworks-catalyzed advanced oxidation processes: A review. J. Hazard. Mater, 372, 3-16. doi:10.1016/j.jhazmat.2017.09.043

Singh, A. K., Bharati, R.C., Manibhushan, N. C., and Pedpati, A. (2013). An assisment of faba bean (*Vicia faba* L.) current status and future prospect. African Journal of Agricultural Research, Vol. 8(50), pp. 6634-6641, 26 December, do: 10.5897/AJAR2013.7335

Tauc, J., Grigorovici, R., Vancu, A. (1966). Optical properties and electronic structure of amorphous germanium. Physica status solidi (b), 15(2), 627-637. doi.org/10.1002/pssb.19660150224

Valente, I. M., Maia, M.R.G., Malushi, N., Oliveira, H.M., Papa, L., Rodrigues, J.A., Fonseca, A.J.M., Cabrita, A.R.J. (2018). Profiling of phenolic compounds and antioxidant properties of European varieties and cultivars of *Vicia faba* L. pods. Phytochemistry, 152, 223–229, doi:10.1016/j.phytochem.2018.05.011

Yakuphanoglu, F. Erten, H. (2005). Refractive index dispersion and analysis of the optical constants' of an ionomer thin flm. Opt Appl, 35(4), 969.

DOI:https//doi.org/10.22452/mjs.vol43no3.3
Malaysian Journal of Science 43(3): 22-29 (September 2024)